Biochimica et Biophysica Acta 1813 (2011) 480–491

Contents lists available at ScienceDirect

Biochimica et Biophysica Acta

journal homepage: www.elsevier.com/locate/bbamcr

Presenilin-1 processing of ErbB4 in fetal type II cells is necessary for control of fetal lung maturation

Kristina Hoeing [a,b,1], Katja Zscheppang [b], Sana Mujahid [c], Sandy Murray [a], MaryAnn V. Volpe [a], Christiane E.L. Dammann [a,b], Heber C. Nielsen [a,b,c,*]

[a] Department of Pediatrics, Floating Hospital for Children at Tufts Medical Center, 800 Washington Street, Box 097, Boston, MA 02111, USA
[b] Department of Pediatrics, Hannover Medical School, Hannover, Niedersachsen, Germany
[c] Department of Anatomy and Cell Biology, Tufts University Sackler School of Biomedical Sciences, Harrison Ave, Boston MA 02111, USA

ARTICLE INFO

Article history:
Received 15 June 2010
Received in revised form 29 November 2010
Accepted 21 December 2010
Available online 29 December 2010

Keywords:
ErbB receptors
Gamma secretase
Yes-associated protein
Fetal lung
Type II cells
Surfactant proteins

ABSTRACT

Maturation of pulmonary fetal type II cells to initiate adequate surfactant production is crucial for postnatal respiratory function. Little is known about specific mechanisms of signal transduction controlling type II cell maturation. The ErbB4 receptor and its ligand neuregulin (NRG) are critical for lung development. ErbB4 is cleaved at the cell membrane by the γ-secretase enzyme complex whose active component is either presenilin-1 (PSEN-1) or presenilin-2. ErbB4 cleavage releases the 80 kDa intracellular domain (4ICD), which associates with chaperone proteins such as YAP (Yes-associated protein) and translocates to the nucleus to regulate gene expression. We hypothesized that PSEN-1 and YAP have a development-specific expression in fetal type II cells and are important for ErbB4 signaling in surfactant production. In primary fetal mouse E16, E17, and E18 type II cells, PSEN-1 and YAP expression increased at E17 and E18 over E16. Subcellular fractionation showed a strong cytosolic and a weaker membrane location of both PSEN-1 and YAP. This was enhanced by NRG stimulation. Co-immunoprecipitations showed ErbB4 associated separately with PSEN-1 and with YAP. Their association, phosphorylation, and co-localization were induced by NRG. Confocal immunofluorescence and nuclear fractionation confirmed these associations in a time-dependent manner after NRG stimulation. Primary ErbB4-deleted E17 type II cells were transfected with a mutant ErbB4 lacking the γ-secretase binding site. When compared to transfection with wild-type ErbB4, the stimulatory effect of NRG on surfactant protein mRNA expression was lost. We conclude that PSEN-1 and YAP have crucial roles in ErbB4 signal transduction during type II cell maturation.

1. Background

1.1. Fetal lung surfactant production

Respiratory distress syndrome (RDS) of the newborn occurs as a result of insufficient surfactant production due to prematurity. Despite the beneficial effects of prenatal glucocorticoids and postnatal surfactant replacement therapies, RDS remains one of the significant causes of morbidity and mortality in premature infants [1,2].

Surfactant synthesis and release take place in the alveolar epithelial type II cells. Type II cell maturation in the fetal lung is under multifactorial control, in which paracrine mesenchymal-type II cell communication mechanisms play a central role. We have shown that the growth factor Neuregulin (NRG-1), which is secreted by fibroblasts, plays a prominent role in this paracrine mesenchymal–epithelial cell communication by stimulating maturation of surfactant synthesis in fetal lung type II cells [3]. NRG is a ligand of the ErbB3 and ErbB4 receptors. We have shown that ErbB4 signaling in fetal type II cells in response to NRG or fetal lung fibroblast conditioned medium (FCM) is a potent stimulator of type II cell maturation and surfactant synthesis [4,5].

1.2. ErbB receptor biology

The ErbB4 receptor is a member of the ErbB family of tyrosine kinase receptors, which also includes ErbB1 (EGF receptor), ErbB2, and ErbB3. All four receptors are transmembrane tyrosine kinase proteins and act as important regulators of cell proliferation and differentiation during fetal organ development, most notably in the

Abbreviations: ActB, beta actin; Cyt, cytosolic; Mem, membrane; Nuc, nuclear

* Corresponding author. Department of Pediatrics, Floating Hospital for Children at Tufts Medical Center, 800 Washington Street, Box 097, Boston, MA 02111, USA. Tel.: +1 617 636 5053; fax: +1 617 636 4233.
E-mail addresses: kristinahoeing@hotmail.de (K. Hoeing), zscheppang.katja@mh-hannover.de (K. Zscheppang), sana.mujahid@tufts.edu (S. Mujahid), smurray1@tuftsmedicalcenter.org (S. Murray), mvolpe1@tuftsmedicalcenter.org (M.V. Volpe), cdammann@tuftsmedicalcenter.org (C.E.L. Dammann), heber.nielsen@tufts.edu (H.C. Nielsen).
[1] Current address: Hannover Medical School, Department of Pediatrics, Carl-Neuberg-Straße 1, 30625 Hannover, Germany. Tel.: +49 5115329007.

0167-4889/$ – see front matter © 2010 Elsevier B.V. All rights reserved.
doi:10.1016/j.bbamcr.2010.12.017

development of the heart and the nervous system [6–9].The importance of ErbB4 in lung development, especially for type II cell maturation, is now becoming evident. ErbB4 is the most prominent dimerization partner in fetal lung type II cells. ErbB4 down regulation in type II cell cultures using siRNA blocks NRG and FCM stimulation of surfactant production. ErbB4 deletion *in vivo* leads to delayed fetal lung development [10] and alveolar simplification, a hyper reactive airway system, and signs of chronic inflammation in the adult lung [11].

ErbB4 signal transduction is a complex process. Binding of NRG in the extracellular ligand binding site causes ErbB4 to form homo- or heterodimers with other ErbB receptors linked by disulfide bonds in the extracellular domain. These receptor dimers then undergo autophosphorylation on tyrosine residues within the intracellular domain. The tyrosine phosphorylation may then activate signal cascades through specific intracellular signaling pathways such as the PI3 kinase/Akt pathway to ultimately influence gene expression. A more recently discovered novel signaling mechanism involves enzymatic cleavage of activated ErbB4 at the intracellular membrane, releasing an 80 kDa intracellular fragment that translocates to the nucleus where it interacts with DNA to directly regulate gene expression. We have reported the presence of ErbB4 in the nucleus of fetal lung type II cells in culture [12]. The signaling mechanisms of ErbB4 in fetal lung type II cells have not been studied.

The novel nuclear trafficking mechanism of ErbB4 signaling is initiated by a two-step cleavage process that is induced by the binding of NRG [13–15]. The initial proteolysis is performed by the transmembrane metalloproteinase TACE (Tumor Necrosis Factor-alpha Converting Enzyme, also known as ADAM 17) [16]. This ectocytic cleavage produces an ectodomain fragment of 120 kDa and a membrane-associated 80 kDa (m80) fragment, which includes the transmembrane and cytoplasmic domains of ErbB4 [17]. The second cleavage step is endocytic cleavage within the transmembrane domain by γ-secretase, releasing the intracellular domain (4ICD) [13,18]. γ-Secretase is an enzyme complex that consists of 4 components. The enzymatically active component is one of the polytopic membrane proteins presenilin-1 (PSEN-1) or presenilin-2 (PSEN-2). The other three identified components are Nicastrin, the Anterior Pharynx Defective-1 (APH-1), and the Presenilin Enhancer Protein (PEN-2). These behave as essential cofactors for PSEN-1 or PSEN-2 [19–25]. The action of γ-secretase alters the ErbB4 m80 fragment to release the soluble s80 fragment 4ICD, which is found in the cytosol and in the nucleus [15,26]. The s80 fragment of ErbB4 associates at least with one chaperon protein, for example, Yes-associated protein (YAP), for transport to the nucleus. YAP was one of the first proteins shown to act as a chaperon protein for ErbB4 [27]. A serine residue in YAP is phosphorylated by the protein kinase Akt, and it subsequently associates with 14-3-3 proteins [28,29]. This binding facilitates the translocation of the ErbB4-YAP-complex from the cytosol to the nucleus [30].

Nuclear localization of ErbB4 is the preferred mechanism of ErbB4 signaling in at least one significant regulatory process during development [31]. We propose that nuclear localization of ErbB4 is important for signaling in type II cell surfactant production. In order to define the mechanisms of nuclear localization of ErbB4 in fetal lung type II cells during development and to determine the role of this signaling pathway in the development of surfactant synthesis, we studied the developmental regulation of PSEN-1 and YAP in fetal mouse type II cells, their activation and association with ErbB4 in response to NRG, and the importance of γ-secretase-mediated ErbB4 nuclear localization for surfactant protein mRNA production. We hypothesized that PSEN-1 and YAP are developmentally regulated in fetal type II cells and that the pathway by which ErbB4 activation in fetal type II cells initiates surfactant protein mRNA production involves activation of PSEN-1 and YAP with nuclear localization of ErbB4.

2. Methods and materials

2.1. Materials

All animal use was approved by the institutional IACUC. Timed-pregnant Swiss Webster Mice were obtained from Taconic Farms (Germantown, NY). Dulbecco's modified Eagle's medium (DMEM), epidermal growth factor (EGF), and monoclonal mouse anti-ß actin (Actb) were purchased from Sigma (St. Louis, MO). Neuregulin 1β (NRG) was kindly provided by Dr. Kermit Carraway III (UC Davis, CA) and purified by Dr. Ann Kane, Phoenix Laboratory (Tufts Medical Center, Boston, MA). Paraformaldehyde was obtained from Fisher Scientific (Fair Lawn, NJ); OCT (optimal cutting temperature embedding medium) was from Miles Laboratories (Elkhardt, IN); Superfrost Plus slides were from Fisher Scientific (Pittsburgh, PA); avidin, biotin, normal goat serum, and alkaline phosphatase chromogen solution were from Vector Laboratories (Burlingame, CA). Alexa Fluor 488 and 568 were obtained from Invitrogen (Carlsbad, CA). Monoclonal mouse anti-PSEN-1 was from Affinity Bio Reagents (Golden, CO). Polyclonal rabbit anti-PSEN-1 and rabbit anti-phospho-PSEN-1 antibodies were obtained from Abcam (Cambridge, MA). Polyclonal rabbit anti-YAP and anti-phospho-YAP antibodies were purchased from Cell Signaling Technology (Danvers, MA). Monoclonal anti-phospho-tyrosine was obtained from Cell Essentials (Boston, MA). Monoclonal mouse anti-YAP and polyclonal rabbit anti-ErbB-4 (C-18) antibodies were from Santa Cruz Biotechnology (Santa Cruz, CA). Monoclonal mouse anti-LAP2 antibody was from BD Transduction Laboratories (San Jose, CA). HRP-linked polyclonal goat anti-rabbit and goat anti-mouse antibodies were from Perkin Elmer Life Science (Boston, MA). Protein A sepharose CL-4B was from Amersham Bioscience (Uppsala, Sweden). Plastic tissue culture dishes, flasks, 6-well and 12-well plates were purchased from BD Bioscience (San Jose, CA). Fetal calf serum (FCS) was from Hyclone (Logan, UT). Hank's balanced salt solution (HBSS) and DNase were from Gibco (Grand Island, NY). BCA™ Protein Assay Reagents were from Thermo Scientific (Rockford, IL). Precision Standards Dual Color and pure nitrocellulose membranes were obtained from Bio-Rad Laboratories (Palo Alto, CA). Nanofectin™ was from PAA-Laboratories (Pasching, Austria). Total RNA Isolation Reagent was from ABgene (Darmstadt, Germany); the forward primers (FP), reverse primers (RP) and probes specific for beta actin (*Actb*), surfactant protein A1 (*Sftpa1*), surfactant protein B (*Sftpb*), surfactant protein C (*Sftpc*), surfactant protein D (*Sftpd*), and the Sftpb promoter were from Eurogentec (Cologne, Germany). TaqMan Universal PCR Master Mix and ABI PRISMTM Big Dye Terminator Cycle Sequencing Ready Reaction Kit were from Applied Biosystems (Darmstadt, Germany). Plasmid Midi Kit was from Qiagen (Hilden, Germany). First-Strand cDNA Synthesis Kit was from Amersham Biotechnologies (Munich, Germany).

2.2. Whole lung immunostaining

PSEN-1 and YAP expression were examined in whole lung sections from fetal mice of gestation E16, E17, and E18 in a modification of methods we have previously described [32]. Briefly, lungs were fixed in PBS (phosphate-buffered saline) containing 4% PFA (paraformaldehyde), pH 7.2, for 4 h and incubated in PBS with 30% sucrose overnight at 4 °C. The lungs were embedded in OCT, cut into 8-μm sections in a cryostat at −21 °C and washed with 100% acetone for 2 min at −21 °C. Several slides were thawed to room temperature and washed for 1 h in sterile filtered PBS containing 0.1% Tween (PBST). All subsequent washes were done in PBST. Non-specific binding was prevented by sequential blocking by avidin (15 min), biotin (15 min), and 1.5% normal goat serum (30 min). Control sections were then incubated with PBS, one group of the experimental samples was incubated with PSEN-1 antibody (1:200), the other group with YAP antibody (1:200) overnight at 4 °C. Next, sections were sequentially incubated with goat anti-rabbit biotinylated

antibody for 60 min, with avidin-blocking complex for 30 min and with alkaline phosphatase for 30 min. After a last washing with distilled H_2O for 10 min, the sections were finally counterstained with Vector fast red and analyzed by light microscopy.

2.3. Mouse type II cell isolation and NRG stimulation

Fetal mouse lung type II cells were isolated and cultured as described before [3]. Briefly, mice were sacrificed with CO_2 inhalation at E16, E17, and E18 of gestation (term = E19). The fetuses were removed. The lungs were transferred into HBSS (Hank's buffered saline solution) on ice, minced into 1 mm^3 pieces, and digested in DMEM (Dulbecco's modified Eagle's medium) containing 0.1% type II collagenase for 2 h at 37 °C and 30 min on ice. The cells were centrifuged at 650×*g* for 5 min at 4 °C, resuspended in DMEM, and incubated on ice for 30 min, followed by a second 650×*g* centrifugation. The cell pellet was dissociated with HBSS containing 0.25% trypsin and DNase (20 μg/ml) for 12 min at 37 °C. This reaction was inhibited by adding DMEM with 10% FCS. The cells were filtered through sterile nitex filters and centrifuged at 650×*g* for 10 min at 4 °C. The pellet was resuspended in DMEM with 10% FCS, and the cells were placed into 100 mm dishes (4–5 lungs/dish) for 1 h at 37 °C to provide a first fibroblast adherence. The supernatant was then centrifuged for 5 min at 4 °C. The pellet was resuspended in DMEM with 10% FCS and placed into T75 flasks (7–8 lungs/flask) for 75 min at 37 °C to allow a second differential adherence step. The medium containing the non-adherent cells was once again removed and centrifuged as described before, resuspended in DMEM with 20% FCS, plated into 12-well plates, and incubated overnight at 37 °C. The non-adhesive cells were gently washed away with PBS. Using staining for lamellar bodies, we have shown 89% purity of fetal mouse type II cells with this culture procedure.

Experiments using NRG administration were conducted when the type II cells appeared 80% confluent. Cells received 33 nM NRG for a 5-min period, except for experiments using confocal microscopy, in which the duration of NRG was as stated in the Results section. The NRG dose is consistent with those commonly used to evaluate acute ErbB4 receptor activation and initiation of signal transduction, and they are referred to hereafter as stimulation experiments.

2.4. Subcellular fractionation

Subcellular fractionation experiments were done as we have described [33]. Briefly, 40 wells each of 12-well plates, untreated and stimulated E17 type II cells, were washed 3 times with ice-cold PBS and scraped in 100 μl homogenization buffer (20 mM Tris–HCl, 250nM sucrose, 1 mM EGTA, 1 mM Dithiothreitol, 1 mM PMSF) containing protease inhibitors (1 μg/ml Pepstatin, 10 μg/ml Leupeptin, 10 μg/ml Phosphoamidon) and phosphatase inhibitor cocktail (250 mM NaF, 200 mM beta-glycerophosphate, 50 mM tetrasodium pyrophosphate, 50 mM Hepes, 25 mM EDTA, distilled H_2O). After 10 passes of sonication, the suspension was centrifuged for 10 min at 800×*g* at 4 °C. The supernatant was further processed to isolate membrane and cytosolic fractions. After centrifugation at 100,000×*g* for 45 min at 4 °C the top layer was transferred into Centricon tubes, centrifuged for 30 min at 5000×*g* at 21 °C and then for 3 min at 750×*g* at 4 °C. The remaining fluid was collected as the cytosolic fraction. The pellets from the original 100,000×*g* centrifugation centrifuge tubes were resuspended in 250 μl of homogenization buffer with all protease inhibitors and 1% Triton X-100 and vortexed vigorously for 1.5 h, followed by centrifugation at 100,000×*g* at 4 °C for 30 min. The supernatant was collected as the membrane fraction. The samples were analyzed by Western blotting. To ensure that we did not lose protein between the centrifugation steps, we measured protein amounts of the supernatants after the 3 main centrifugation steps (10-min centrifugation, 45-min centrifugation, and purified samples). In total the protein loss was less than 3%.

2.5. Co-immunoprecipitation and Western blotting

At 80% confluence, the cells were serum starved for 3 h, stimulated for 5 min with NRG (33nM) or with DMEM (untreated). The cells were washed with ice-cold PBS and harvested in co-immunoprecipitation buffer (20 mM Tris (pH 7.4), 150 mM NaCl, 1 mM $MgCl_2$, 1% Triton X-100, 10% Glycerol, 1 mM Na_3Vo_4, 1 mM NaF, 1 mM $ZnCl_2$, 10 mM beta-glycerol-phosphate, 5 mM tetrasodium pyrophosphate, 1 mM PMSF, 4 μg/ml each of aprotinin, leupeptin, pepstatin). Aliquots (200 μg protein) of whole cell lysates were incubated with the specific antibody (PSEN-1 or YAP) for 1.5 h at 4 °C. After adding Protein-A Sepharose, the sample was incubated with gentle rocking over night at 4 °C. The following day, the beads were washed 3 times with co-immunoprecipitation washing buffer (20 mM Hepes (ph7.4), 150nM NaCl, 1 mM EDTA, 1% Triton X-100, 1 mM Na_3VO_4, 1 mM NaF, 10 mM beta-glycerol phosphate, 5 mM tetrasodium pyrophosphate, 1 mM PMSF and 4 μg/ml each of aprotinin, leupeptin, and pepstatin) and between washes microcentrifuged at 100×*g* at 4 °C for 10 min. The supernatant was removed into Laemmli buffer for 5 min at 100 °C. The proteins were separated using an 8% SDS-gel and transferred to nitrocellulose membranes. The blots were stained with Ponceau's to confirm efficient transfer. After blocking in 1% BSA in TBST for 1 h, the membranes were incubated with anti-phospho-tyrosine, anti-phospho-YAP, anti-phospho-PSEN-1, anti-ErbB4, anti-YAP, and anti-PSEN-1 antibodies overnight at 4 °C. The proteins were visualized by enhanced chemiluminescence.

2.6. Confocal microscopy

Type II cells from E17 mice were cultured on glass cover slips. After 3 h of serum starvation, the cells were incubated with DMEM (untreated) or stimulated for 5 min, 30 min and 24 h with NRG (33nM), then prepared for confocal imaging. Cells were washed with PBS; all subsequent washes were done with PBS. Cells were fixed for 20 min with 3% PFA (pH 7.2), permeabilized with PBS containing 0.5% Triton X-100 for 5 min at 4 °C, and blocked with 10% normal goat serum for 1 h. After further incubating with primary antibody against PSEN-1 or YAP plus ErbB4 antibody for 30 min at room temperature, cells were incubated with secondary antibodies with fluorochrome labels (Alexa 488 and 568) for 30 min at room temperature in the dark. Finally, the cells were incubated with DAPI containing mounting medium over night at room temperature. Cells were analyzed using a Leica TCS-SP2 confocal laser scanning microscope.

2.7. Nuclear fractionation

For nuclear fractionation, untreated and stimulated (5 min, 30 min, 24 h) E17 type II cells were lysed in nuclei buffer (pH 7.9, 10 mM HEPES, 1.5 mM MgCl2, 10 mM KCl, 1% Triton X-100, 0.5 mM DTT) as described before [34]. The suspension was kept on ice for 10 min and centrifuged at 10,000×*g* at 4 °C for 10 min. The supernatants (cytoplasmic fractions) were stored at −80 °C and the pellets (containing the nuclear fractions) were suspended in High Salt Buffer (pH 7.9, 10 mM HEPES, 400 mM NaCl, 0.1 mM EDTA, 5% glycerol, 0.5 mM DTT), kept on ice for 20 min, and centrifuged at 10,000×*g* at 4 °C for 10 min. The final supernatants (nuclear fractions) were stored at −80 °C until further use. Proteins of the different cell fractions were analyzed by Western blotting and probed for the 80 kDa ErbB4 fragment (4ICD), YAP, Lap2 (a nuclear marker), and for ActB as an internal standard.

2.8. Cell transfection

Type II cells were cultured in 6-well plates for 24 h at a cell density of 1×10^6 cells/ml. Transfections were performed as described by the manufacturer. Briefly, 1 μg DNA of pEGFP N3 (control plasmid), pHER4 GFP (full-length ErbB4 receptor), or pHER4V673IMU (mutant, defective in the γ-secretase binding site) was diluted with Nanofectin transfection reagent and incubated for 30 min before it was added drop-wise into the serum-containing medium. Cells were harvested after 48 h of transfection for real-time PCR.

2.9. RNA isolation and cDNA synthesis

After transfection cells were lysed in RNA isolation reagent. RNA was isolated by acid phenol/chloroform extraction [35]. Five micrograms of total RNA was used for reverse transcription using a cDNA synthesis kit (GE Healthcare) in a 15 μl reaction volume containing 1× DTT, 0.2 μg hexamer primer, and 5× bulk mix for 1 h. The resulting cDNA was used for real-time amplification reactions.

2.10. Quantitative real-time PCR

The cDNA levels for *Sftpa1*, *Sftpb*, *Sftpc*, *Sftpd*, and *Actb* gene transcripts were measured by real-time PCR as previously described [11]. Actb was used as an internal control to normalize the surfactant protein cDNA levels. The 20 μl reaction mixture contained 1 μl of the cDNA template, 10 μl TaqMan universal master mix (Applied Biosystems), 300 nM each of forward and reverse primer, and 200 nM probe. For amplification and detection of specific products, the ABI PRISM 7500 sequence detection system was used (Applied Biosystems). The amplification protocol consisted of an initial denaturation and enzyme activation at 95 °C for 10 min, followed by 45 cycles at 95 °C for 15 s and 60 °C for 1 min. The threshold cycle was determined for each gene [36]. Samples were run in quadruplicates. The method of Seiffert et al. was used to estimate the relative expression level of the surfactant protein genes by calculating the DCt value, representing the difference in the Ct values of the target and the reference gene [37]. The differences in the Ct values of the ErbB4 transfected cells compared to cells transfected with the EGFP control plasmid were calculated as DDCt and represented as $DDCt^{-1}$ (DDCt values are inversely proportional to the levels of Sftp mRNA). For each assay, specificity was confirmed by sequencing the PCR products on both strands using capillary electrophoresis with POP-6TM-Polymer on an ABI 3100 Genetic Analyzer (Applied Biosystems).

2.11. Data analysis

All data are presented as mean ± SEM of experimental-specific controls unless otherwise stated. Two-tailed *t*-tests were used to evaluate the results for statistical significance, using the Instat statistical package (GraphPad Software, San Diego, CA).

3. Results

3.1. Cell-specific expression of PSEN-1 and YAP

Immunohistochemistry showed changes with gestation in both PSEN-1 and YAP immunolocalization in E16, E17, and E18 female fetal mouse lungs (Fig. 1). At E16 (Fig. 1B) PSEN-1 protein was weakly seen in cytoplasm of cuboidal epithelium and in surrounding mesenchyme. The columnar epithelium of bronchiolar airways (asterisk) was negative. PSEN-1 expression at E17 (Fig. 1C) and E18 (Fig. 1D) was increased in cuboidal epithelium and in the epithelium at the transition from distal bronchioles to alveolar ducts (asterisk in Fig. 1C), compared to E16 lung sections. Mesenchymal cells adjacent to cuboidal epithelium were also strongly positive but clusters of mesenchymal cells between the airways were less positive. YAP staining was weak at E16 (Fig. 1E), changing to a strong expression at E17 (Fig. 1F) and E18 (Fig. 1G) in cuboidal epithelium, particularly at the tips of alveolar ducts. Low cuboidal epithelium (asterisk in 1F) was also positive at E17 and E18. YAP staining was minimally present in mesenchyme (arrowheads in Fig. 1F and G).

3.2. Gestational regulation of PSEN-1 and YAP protein expression

Western blotting of whole cell lysates was used to identify the gestational regulation and the effect of NRG on PSEN-1 and YAP (Fig. 2A). Gestational regulation was identified by expressing the densitometry values of unstimulated (no NRG) E17 and E18 results as a percent of baseline E16. The effects of NRG stimulation were evaluated by comparing the changes of protein expression on densitometry to the endogenous expression of their respective gestation-specific unstimulated controls. PSEN-1 exhibited a strong gestational increase in E17 type II cells to 181% ± 17% (mean ± SE, $p=0.0006$, $n=6$) and in E18 type II cells to 172% ± 20% (mean ± SE, $p=0.007$, $n=6$) compared with E16 cells (100% ± 1%, $n=6$) (left panel, Fig. 2B). The development of YAP expression in type II cells showed patterns of gestational regulation and NRG effects quite similar to that of PSEN-1. Endogenous YAP baseline expression was increased to 243% ± 35% in E17 type II cells (mean ± SE, $p=0.002$, $n=4$) and to 207% ± 29% in E18 type II cells (mean ± SE, $p=0.004$, $n=4$) compared to E16 cells (100% ± 1%, $n=4$) (right panel, Fig. 2B). Five-minute stimulation with NRG did not significantly change the amount of PSEN-1 on any day (E16 100% ± 6%; mean ± SE, $p=0.9$, $n=3$; E17 99% ± 10%; mean ± SE, $p=0.9$, $n=3$; E18 104% ± 13%; mean ± SE, $p=0.7$, $n=3$), or the amount of YAP (E16 97% ± 5%; mean ± SE, $p=0.4$, $n=3$; E17 108% ± 8%; mean ± SE, $p=0.3$, $n=3$; E18 99% ± 7%; mean ± SE, $p=0.9$, $n=4$).

3.3. Cellular distribution of PSEN-1 and YAP

We performed subcellular fractionations to determine the cellular distribution of PSEN-1 and YAP at baseline and after NRG stimulation (Fig. 3A). We measured the amount of protein in the cytosolic fraction using ActB as an internal standard. Although some Actb is necessarily found in the membrane fraction, we were not confident that this would be a consistent proportion. Therefore, we quantified the membrane fraction as the ratio between the membrane protein and the Actb-standardized cytosolic protein. As would be expected, PSEN-1 and YAP were present in the membrane and more prominently in the cytosolic fractions. In NRG-stimulated cells, the membrane/cytosol ratio of PSEN-1 was significantly increased to 144% ± 12% (mean ± SE, $p=0.02$, $n=3$) in E17 type II cells and to 140% ± 16% (mean ± SE, $p=0.01$ $n=3$) in E18 cells compared to their gestational specific unstimulated ratios. NRG also induced an increase of the YAP membrane/cytosol ratio in E17 cells (121% ± 12%; mean ± SE, $p=0.03$, $n=3$), and in E18 cells (125% ± 13%; mean ± SE, $p=0.02$, $n=3$), suggesting a relocation of PSEN-1 and YAP to the membrane with NRG stimulation. This effect was not seen in E16 cells for either the PSEN-1 membrane/cytosol ratio (103% ± 5%; mean ± SE, $p=0.7$, $n=3$) or the YAP membrane/cytosol ratio (103% ± 2%; mean ± SE, $p=0.1$ $n=3$) (Fig. 3B).

3.4. Effects of NRG on cellular localization and co-localization of ErbB4 with PSEN-1 and ErbB4 with YAP

Confocal microscopy was used to confirm the subcellular fractionation results and to learn more about cellular co-localization of ErbB4 with both PSEN-1 and YAP. As we have previously reported [12], ErbB4 (red) at baseline was found at the cell membrane, within the cytoplasm and diffusely in the nucleus. PSEN-1 (green) at baseline was primarily seen in the nucleus and more weakly in the cytoplasm

(Fig. 4A). After a 5-min NRG stimulation, both PSEN-1 and ErbB4 were more prominent in the perinuclear region and in the nucleus. Although the nuclear ErbB4 signal in Fig. 4A is less strong than at baseline, we have shown in several papers that nuclear ErbB4 is strong after 5 min of NRG stimulation (see also Fig. 4B) [12] [4]. However, the important finding in this figure, which is also consistent with all our

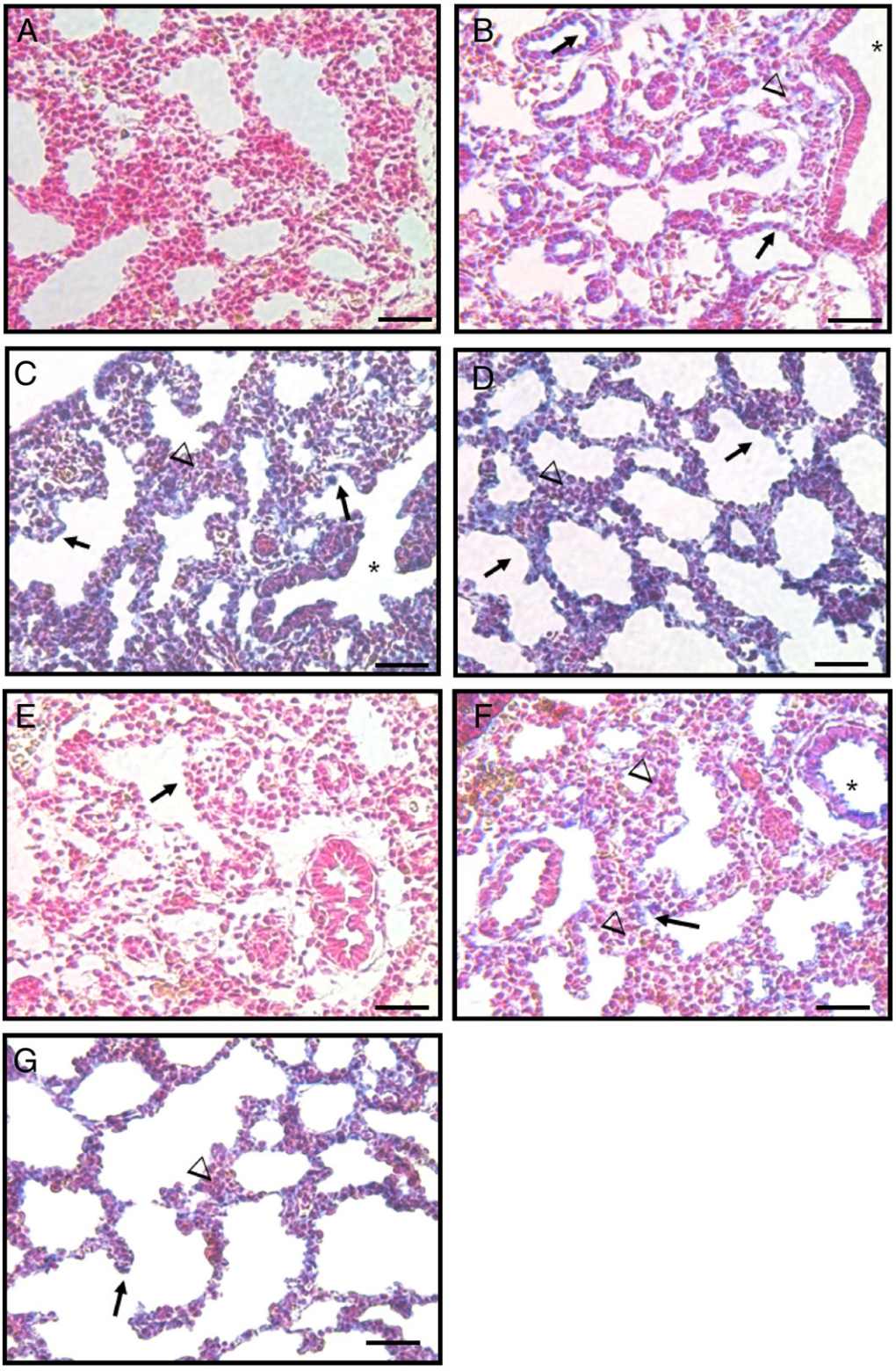

Fig. 1. PSEN-1 and YAP immunohistochemistry in E16, E17, and E18 fetal mouse lungs. In the absence of primary antibody (A), no blue staining is seen. At E16 (B), PSEN-1 protein is seen in the cytoplasm of the cuboidal epithelium (arrows in B) and in surrounding mesenchyme (arrowheads). However, columnar epithelia of bronchiolar airways (asterisk) are negative. Expression of PSEN-1 at E17 (C) and E18 (D) increases in cuboidal epithelium (arrows) and epithelium of distal bronchioles (asterisk in C) at the entrance to alveolar ducts. Mesenchymal cells adjacent to cuboidal epithelium are also strongly positive but clusters of mesenchymal cells between airways (arrowheads in C and D) are less positive, specifically in E18 (D). YAP cellular expression is minimal at E16 (E), but at E17 (F) and E18 (G), expression is present in cuboidal epithelium (arrows) particularly at tips of alveolar ducts. Low cuboidal epithelium (asterisk) is also positive at E17 and E18. Minimal YAP staining is present in mesenchyme (arrowheads in F and G). Scale bars are 50 μm.

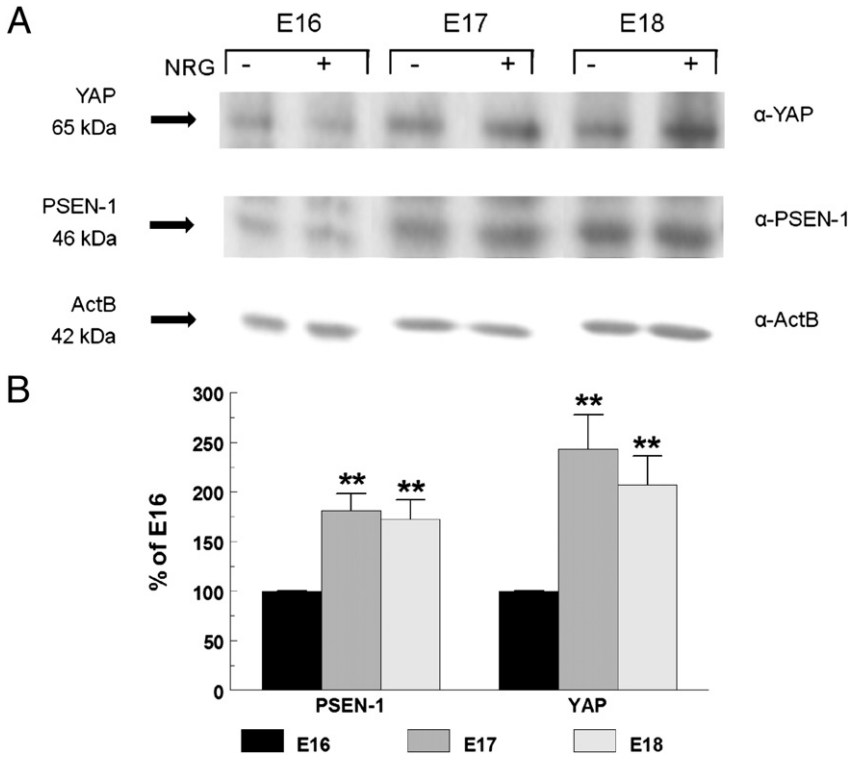

Fig. 2. Gestational age-specific expression of PSEN-1 and YAP. (A) Western blot of whole cell lysates of E16, E17, and E18 type II cells, unstimulated and stimulated with NRG (33nM), probed for YAP (65 kDa), PSEN-1(46 kDa), and beta actin (ActB) (42 kDa) (B). Densitometry of PSEN-1 and YAP expression in whole type II cell lysates. PSEN-1 expression (left group) is significantly increased at E17 (dark grey bar) ($^{**}p<0.0006$, $n=6$) and E18 (light grey bar) ($^{**}p<0.007$, $n=6$) compared to E16 (black bar) ($n=6$). YAP expression (right group) also is significantly increased at E17 ($^{**}p<0.002$, $n=4$) and E18 ($^{**}p<0.004$, $n=4$) compared to E16 ($n=4$) cells.

previous work, is the perinuclear concentration of ErbB4. After 30 min of stimulation, PSEN-1 was concentrated in the cytoplasm and in the nucleus; ErbB4 was found in the same regions and in the cell membrane. The overlay showed an increasing co-localization in the perinuclear area immediately after the 5-min stimulation. After 30 min co-localization was strong in the nucleus. After 24 h of NRG

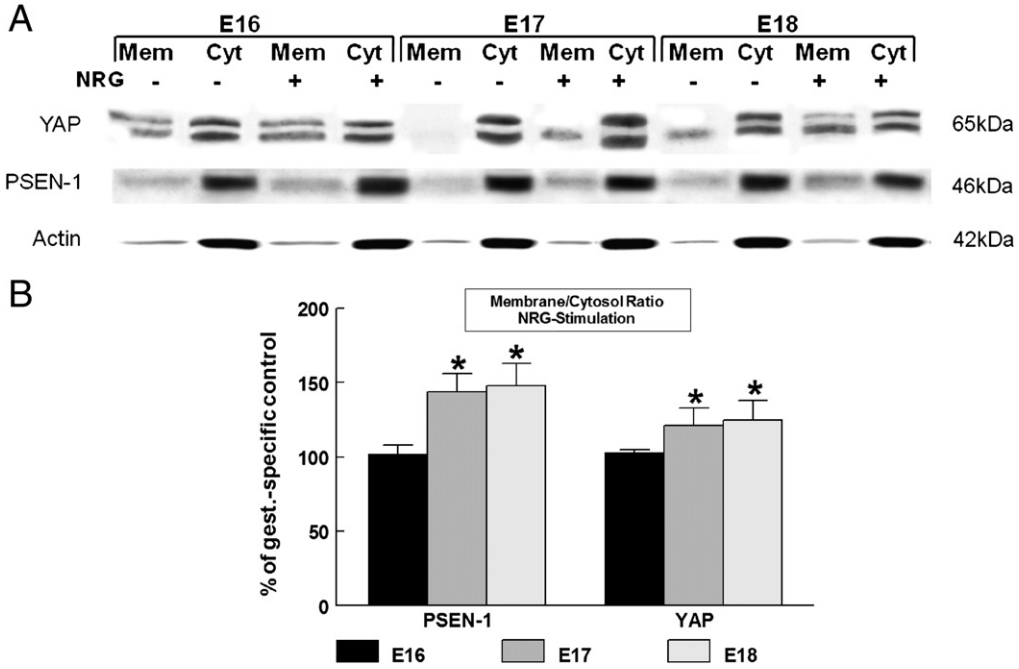

Fig. 3. Gestational age-specific subcellular localization of PSEN-1 and YAP. (A) Representative Western blot of the subcellular fractionation of E16, E17, and E18 type II cells. Untreated cells (NRG−) and NRG-stimulated (NRG+) cells were probed for anti-YAP (65 kDa), anti-PSEN-1 (46 kDa), and anti-Actb antibodies (42 kDa). PSEN-1 and YAP are strongly expressed in the unstimulated and stimulated cytosolic fraction (cyt). With NRG stimulation, there is an increase of expression of both proteins in the membrane fraction (mem) compared to unstimulated membrane Fractions. (B) Densitometry analysis shows the quantification of NRG-induced PSEN-1 and YAP expression in the membrane–cytosol ratios. NRG stimulation caused an increase in the membrane–cytosol ratio of PSEN-1 in E17 ($^{*}p<0.02$, $n=3$) and E18 ($^{*}p<0.01$ $n=3$) type II cells compared to their gestational specific controls. The membrane–cytosol ratio of YAP is also significantly increased in E17 ($^{*}p<0.03$, $n=3$) and E18 ($^{*}p<0.02$, $n=3$) type II cells.

stimulation PSEN-1 was seen in the nucleus and in specific perinuclear areas, whereas ErbB4 localization was additionally present in the cell membrane. However, the overlay exhibited weak co-localization in the nucleus and perinuclear areas compared to earlier time points (Fig. 4A).

The localization of YAP and its pattern of co-localization with ErbB4 differed from PSEN-1 (Fig. 4B). At baseline, YAP (green) showed a nuclear and a scattered cytoplasmic signal. Those regions showed light co-localization with ErbB4 in the overlay. We observed a prominent nuclear and punctuate cytoplasmic YAP localization after 5 min of stimulation. At 30 min a diffuse weak YAP signal was present in the cytoplasm and membrane, while the nuclear signal remained strong. After 24 h YAP had resumed its baseline pattern. The overlay exhibited a prominent perinuclear and nuclear co-localization at 5 min of stimulation, which diminished after 30 min and was faint after 24 h.

3.5. Time course of YAP nuclear re-localization

The observation that YAP precipitated the 4ICD more than the full-length ErbB4 after NRG stimulation prompted us to investigate the time course of nuclear localization of the ErbB4 fragment and YAP. Nuclear fractionation experiments were performed with fetal type II cells untreated and stimulated for 5 min, 30 min, and 24 h. Western blots were probed for the ErbB4 fragment, YAP, Lap2 (a nuclear lamina protein [38]), and beta actin (Fig. 4C). The 4ICD fragment was mainly present in the nucleus. Comparing untreated and stimulated nuclear fractions, we noticed the greatest difference in the 4ICD fragment after 5 min of stimulation, indicating a 4ICD movement towards the nucleus after short stimulation. YAP was mainly present in the cytoplasm; however, a smaller amount was permanently present in the nucleus. Nuclear YAP was also highest at 5 min stimulation and diminished after 30 min and 24 h. Lap 2 appeared only in the nucleus, confirming a clean fractionation.

3.6. Co-precipitation of ErbB4 with PSEN-1 and YAP

Confocal co-localization experiments do not confirm protein–protein association or interaction. Therefore, co-immunoprecipitation experiments were used to assess interactions between PSEN-1 and ErbB4 and YAP and ErbB4 in E17 type II cells. For PSEN-1 and ErbB4, cell lysates were immunoprecipitated with anti-PSEN-1 antibody under co-immunoprecipitation conditions, then probed to detect both PSEN-1 and ErbB4. Both the full-length ErbB4 and the 4ICD fragment co-immunoprecipitated with PSEN-1 (Fig. 5A, representative of 4 experiments), indicating that PSEN-1 associates with ErbB4. Stimulation with NRG enhanced this association, which appeared stronger for the full-length ErbB4 than for the 4ICD. To assess the co-activation (i.e., phosphorylation) of ErbB4 and PSEN-1, we probed the blots with anti-phospho-tyrosine and anti-phospho-PSEN-1 antibodies. As expected, NRG induced phosphorylation of both ErbB4 and PSEN-1. We further probed these immunoprecipitants with anti-YAP antibody but did not find any evidence of YAP pull down (Supplemental Figure 1A). The specificity of the co-immunoprecipitation reaction was verified by simultaneous immunoprecipitations using anti-mouse-IgG probed for anti-phospho-tyrosine, anti-ErbB4, anti-phospho-PSEN-1, and anti-PSEN-1 antibodies. The IgG antibody did not co-immunoprecipitate any of these proteins (Fig. 5A).

Co-immunoprecipitation with anti-YAP antibody was also used to examine YAP–ErbB4 interactions. We found that YAP also co-precipitated full-length ErbB4 and its 4ICD fragment, especially in NRG-stimulated cells. Similar to the PSEN-1 co-immunoprecipitation results, NRG induced both ErbB4 phosphorylation and phosphorylation of YAP in E17 type II cells (Fig. 5B, representative of 5 experiments). Densitometry was done on the YAP experiments to document NRG-induced phosphorylation of the 80 kDa fragment 4ICD associated with activated YAP. For each protein, the NRG condition was expressed as the percent of the control condition. As expected, after NRG stimulation, there was no increase in the amount of immunoprecipitated YAP ($103\% \pm 9\%$; mean ± SE, $p = 0.57$, $n = 5$). There was also no increase of the full-length ErbB4 ($103\% \pm 26\%$; mean ± SE, $p = 0.82$, $n = 5$) nor of its phosphorylation ($125\% \pm 20\%$; mean ± SE, $p = 0.10$, $n = 5$). The densitometry confirmed NRG activation of YAP phosphorylation ($159\% \pm 7\%$; mean ± SE, $p = 0.016$, $n = 5$), increased amount of the 80 kDa 4ICD with NRG ($140\% \pm 29\%$; mean ± SE, $p = 0.08$, $n = 3$), and increased phosphorylation of the 80 kDa 4ICD ($135\% \pm 21\%$; mean ± SE, $p = 0.006$, $n = 5$). These results indicate, first, that YAP associates with both the full-length ErbB4 and the intracellular ErbB4 4ICD fragment and, second, that YAP association with the 4ICD fragment is significantly enhanced by NRG stimulation. Whether this represents association with ErbB4 before its endocytic cleavage by presenilin or separate associations with an intracellularly located full-length ErbB4 and with the 4ICD is not evident. We also probed the YAP immunoprecipitant with anti-PSEN-1 antibody. In agreement with the PSEN-1 co-immunoprecipitation study, YAP immunoprecipitation did not pull down PSEN-1 (Supplemental Figure 1B). Again, immunoprecipitations using anti-rabbit-IgG confirmed the specificity of the YAP co-immunoprecipitation (Fig. 5B).

3.7. Role of γ-secretase in ErbB4 stimulation of surfactant protein mRNA expression

We used transgenic ErbB4 deleted mice ($HER4^{heart}$ (−/−)), in which the embryos are rescued from the lethal cardiac defects by the expression of a transgene containing the human ErbB4 (HER4) gene under control of a cardiac-specific alpha myosin heavy chain promoter (α-MHC) [39], to test the role of γ-secretase processing of ErbB4 in ErbB4-mediated stimulation of fetal surfactant synthesis. Primary cultures of fetal E17 $HER4^{heart}$ (−/−) type II cells (ErbB4-naive type II cells) were transfected with a plasmid expressing wild-type human ErbB4 receptor or a control plasmid (EGFP). Expression of wild-type ErbB4 (HER4) in the ErbB4 naïve $HER4^{heart}$ (−/−) type II cells led to a significant increase in *Sftpa1* (0.6 ± 0.2, mean ± SE, $p = 0.01$, $n = 4$), *Sftpb* (0.9 ± 0.1, mean ± SE, $p = 0.0001$, $n = 3$), *Sftpc* (0.3 ± 0.1, mean ± SE, $p = 0.01$, $n = 4$), and *Sftpd* (1.2 ± 0.2, mean ± SE, $p = 0.0001$, $n = 4$) mRNA levels (black bar) compared to cells transfected with the EGFP control plasmid. Transfection of $HER4^{heart}$

Fig. 4. Co-localization of PSEN-1 and YAP with ErbB4 after NRG stimulation. (A) NRG stimulation induces cellular co-localization of ErbB4 with PSEN-1. At baseline (untreated; time zero), ErbB4 (red) is present in the cell membrane and diffusely in the nucleus. ErbB4 localization changed to a more perinuclear presence (5 min, 30 min) with reappearance at the cell membrane (30 min). At 24 h ErbB4 localization resembles the baseline pattern. PSEN-1 (green) is initially punctate in the cytoplasm and strong in the nucleus. Following NRG stimulation, PSEN-1 is increased in the perinuclear cytoplasm (5 min), which weakens at 30 min but again becomes evident at 24 h. The overlay shows NRG stimulation induces strong co-localization of PSEN-1 and ErbB4 in the perinuclear area (5 min) and within the nucleus at 30 min. Co-localization has mostly disappeared at 24 h. (B) NRG stimulation induces co-localization of ErbB4 with YAP. At baseline YAP (green) is present in the nucleus, the cytoplasm, and the cell membrane. Following NRG stimulation, YAP has become more prominent in the nucleus and punctuate in the perinuclear cytoplasm (5 min). At 30 min YAP is predominantly within the nucleus. It returns to the baseline pattern at 24 h. The overlay shows minimal co-localization of YAP with ErbB4 at time zero. This is followed by pronounced co-localization in the perinuclear cytoplasm and the cell membrane after 5 min of stimulation. After 30 min, there is co-localization in the nucleus and cell surface, which continues at 24 h. (C) Time course of YAP nuclear localization. NRG stimulation enhanced nuclear localization of 4ICD and YAP. Nuclear fractionation experiments with fetal type II cells were untreated and stimulated for 5 min, 30 min, and 24 h. Western blots were probed for the ErbB4 fragment, YAP, Lap2 (a nuclear lamina protein), and Actb. The 4ICD fragment, mainly present in the nucleus, showed the greatest difference in protein amount after 5-min stimulation. YAP, mainly present in the cytoplasm, showed highest nuclear YAP concentration at 5-min stimulation and diminished after that. Lap 2 appeared only in the nucleus, confirming a clean fractionation.

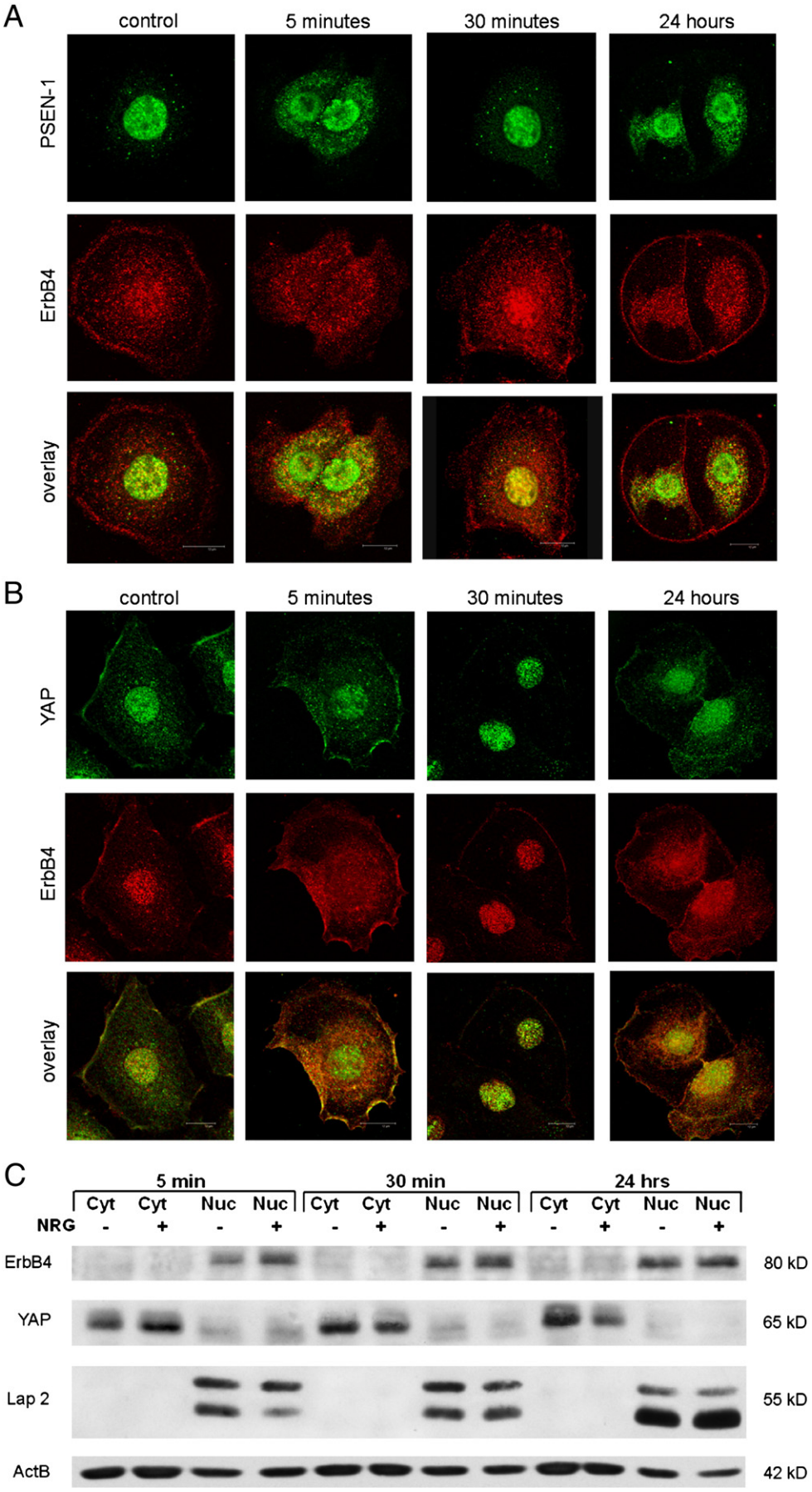
A
control
5 minutes
30 minutes
24 hours
PSEN-1
ErbB4
overlay
B
control
5 minutes
30 minutes
24 hours
YAP
ErbB4
overlay
C
5 min
30 min
24 hrs
Cyt Cyt Nuc Nuc Cyt Cyt Nuc Nuc Cyt Cyt Nuc Nuc
NRG - + - + - + - + - + - +
ErbB4
YAP
Lap 2
ActB
80 kD
65 kD
55 kD
42 kD

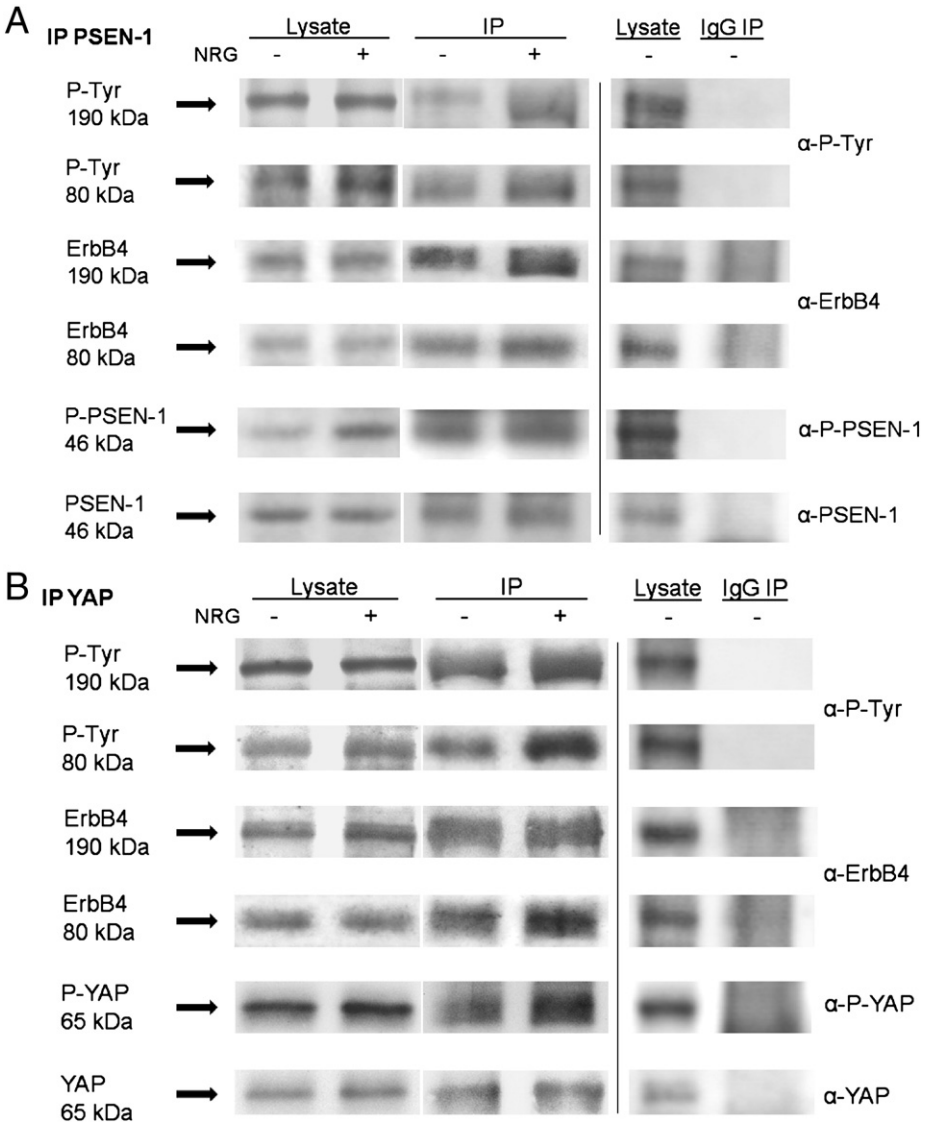

Fig. 5. ErbB4 co-precipitated with PSEN-1 and with YAP. Representative blots of co-immunoprecipitations demonstrating interactions of full-length ErbB4 (190 kDa) and its intracellular domain (80 kDa) with (A) PSEN-1 and (B) YAP were studied in unstimulated (NRG−) and NRG-stimulated (NRG+, 5 min) E17 fetal type II cells, using co-immunoprecipitation conditions. Protein interactions were analyzed by Western blotting. The left two lanes show the cell lysates, the middle two lanes show the specific PSEN-1 and YAP immunoprecipitations, and the right two lanes show unstimulated cell lysates and immunoprecipitations using anti-mouse-IgG (negative control for PSEN-1) and anti-rabbit-IgG (negative control for YAP). Blots of PSEN-1 co-immunoprecipitation and IgG co-immunoprecipitations were probed with anti-phospho-tyrosine, anti-ErbB4, anti-phospho-PSEN-1, and anti-PSEN-1 antibodies. PSEN-1 co-precipitated full-length ErbB4 and its intracellular fragment. This interaction was increased by NRG stimulation. NRG induced phosphorylation of both ErbB4 and PSEN-1. Blots of YAP co-immunoprecipitation and IgG co-immunoprecipitations were reprobed with anti-phospho-tyrosine, anti-ErbB4, anti-phospho-YAP, and anti-YAP antibodies. YAP co-precipitated full-length ErbB4 and its intracellular fragment in fetal type II cells. This interaction was increased by NRG stimulation. NRG induced phosphorylation of both ErbB4 and YAP. Quantitative data for the YAP co-immunoprecipitations are given in the text. Neither IgG co-immunoprecipitations (A and B) pulled down any of the proteins.

(−/−) type II cells with an ErbB4 mutant lacking the γ-secretase binding side (HER4 V673IMu) was associated with significantly decreased *Sftpa1* (-0.7 ± 0.2, mean ± SE, $p = 0.0003$, $n = 3$), *Sftpb* (-0.3 ± 0.1, mean ± SE, $p = 0.0014$, $n = 3$), and *Sftpd* (-0.1 ± 0.2, mean ± SE $p = 0.0024$, $n = 3$) mRNA levels compared to the increased Sftp mRNA abundance in wild-type ErbB4 (HER4) transfected cells. Thus γ-secretase processing of ErbB4 is critical for *Sftpa1*, *Sftpb*, *and Sftpd* expression in the fetal type II cell. We found no significant change in *Sftpc* mRNA expression after transfection with the mutant ErbB4 (HER4 V673IMu) construct (-0.3 ± 0.1 mean ± SE, $p = 0.9$, $n = 3$) compared to the wild-type ErbB4 transfected cells (Fig. 6).

4. Discussion

In spite of advances in the prevention of RDS including the use prenatal glucocorticoids and neonatal treatment with postnatal surfactant replacement, RDS remains one of the significant causes of morbidity and mortality in premature infants [1,2]. Thus, it is important to develop new insights into endogenous pathways regulating the development of surfactant synthesis. We have shown the important role of ErbB4 receptors and NRG for surfactant production [3,4,10], but their specific signaling mechanism(s) in type II cells to promote maturation and surfactant synthesis is not understood. We are motivated to determine ErbB4 signaling and trafficking mechanisms controlling fetal type II cell maturation and surfactant production to provide a foundation for defining new therapeutic approaches to prevent and treat RDS.

The aim of this current study was to define the role of proteins involved in ErbB4 processing and show that processing is needed for stimulation of surfactant protein gene expression. We concentrated on the γ-secretase cleavage step as that is the final step in releasing the 4ICD fragment that traffics to the nucleus [13,18]. There are

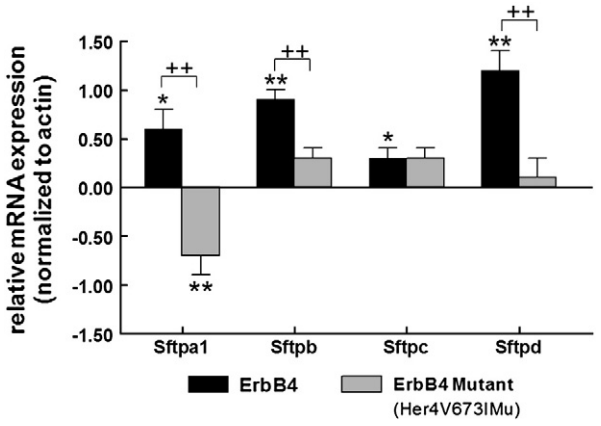

Fig. 6. γ-Secretase activity is required for ErbB4-induced stimulation of surfactant protein (SP) mRNA expression. ErbB4-naive E17 type II cells isolated from HER4^{heart} (−/−) animals were transfected with full-length human ErbB4 (HER4; black bars) or an ErbB4 mutant lacking the γ-secretase binding side (HER4V673IMu; grey bars) and the effect on Sftp expression was measured by quantitative real time PCR. Introduction of ErbB4 into these ErbB4 (−/−) type II cells induced a significant increase in *Sftpa1* ($^{*}p=0.01$, $n=4$), *Sftpb* ($^{**}p<0.0001$, $n=3$), *Sftpc* ($^{*}p=0.01$, $n=4$), and *Sftpd* ($^{**}p<0.0001$, $n=4$) mRNA levels. Preventing γ-secretase-dependent cleavage of ErbB4 significantly inhibited the stimulatory effect of ErbB4 on *Sftpa1* ($^{++}p=0.0003$, $n=3$), *Sftpb* ($^{++}p=0.0014$, $n=3$), and *Sftpd* ($^{++}p=0.0024$, $n=3$) mRNA levels.

two separate enzymes that may make up the active component in the γ-secretase complex, PSEN-1 and PSEN-2, which are transcribed from different genes. Knockout mice of each exhibit pulmonary phenotypes [40,41]. While there is some overlap in their function, studies show that γ-secretase complexes containing PSEN-1 or PSEN-2 have functionally distinct phenotypes [42,43]. The pulmonary phenotype of the PSEN-1 knockout consists of poorly developed alveoli and neonatal death with poorly expanded lungs, while the lungs of PSEN-2 knockout mice develop alveolar wall thickening, alveolar and airway fibrosis, and hemorrhage. Double knockouts show an exacerbation of the fetal/neonatal abnormalities of alveolar development. However, no study has addressed the role of presenilins in signaling for type II cell maturation and surfactant protein expression.

Our focus on PSEN-1 in this study was motivated by the more severe developmental phenotype of alveolar maturation in the PSEN-1 knockout mouse. We also studied the shuttle protein YAP based on the facts that it was one of the first ErbB4 shuttle proteins described and that YAP knockouts are embryonic lethal, preventing any prior analysis of its importance for lung development [30,44]. We performed studies of protein expression and cellular distribution in E16, E17, and E18 fetal mice type II cells, representing the development from the late stage of bronchial branching (late pseudoglandular stage, E16) through the canalicular into the saccular stage of lung development. During this interval in mouse lung development surfactant synthesis is initiated (E17) with subsequent progression to a differentiated alveolar epithelium, which synthesizes surfactant proteins in abundant quantities [45].

Immunohistochemistry of fetal mouse lungs showed that PSEN-1 and YAP are primarily located in lung epithelial cells, with increasing expression as term gestation approached. The localization pattern changed from the epithelial cells of larger airways at E16 to a pronounced saccular expression at E18 of gestation. The analysis of total protein expression of PSEN-1 and YAP in E16, E17, and E18 primary cultures of type II cells was consistent with those results. This developmental pattern reflects that of fetal mouse type II cell maturation, in which E17 is the time when surfactant production begins and E18 when surfactant synthesis is well established.

Evaluation of the acute effects of NRG on cellular PSEN-1 and YAP membrane and cytosolic content after NRG stimulation afforded the opportunity to evaluate the initiation of this ErbB4 processing pathway. Again, baseline results for PSEN-1 and YAP were consistent with former findings. The cytosolic PSEN-1 and YAP content were highest at E17 and E18. NRG stimulation promoted relocalization of these two proteins at E17, suggesting involvement of this signaling pathway in the maturational process. We recognize that the membrane fraction includes membranes from multiple cell compartments, meaning that this crude subcellular fraction gives limited information about the exact subcellular compartment localization. Nevertheless, the results indicate that NRG induces translocation of both PSEN-1 and YAP from the cytosolic to one or more membrane compartments.

We used confocal microscopy to obtain additional insight into the localization of PSEN-1 and YAP and the compartments where they co-localize with ErbB4. Therein, we recognized a constant nuclear staining of PSEN-1 in addition to a cytosolic signal. Nuclear localization of presenilins has been reported in several studies [46–49]. It is clear from our data that in NRG-stimulated fetal type II cells PSEN-1 associates with ErbB4 in the cytosol and the nucleus at different time points. The transport mechanisms of the more than 40 proteins known to interact with PSEN-1 and/or the γ-secretase complex are poorly understood [50–52]. The traditional model suggests that substrate protein–γ-secretase interactions occur at the cell membrane; however, more recent studies bring this into question, suggesting interactions in several cellular compartments [53,54]. Overall, our data are consistent with recent studies addressing the internalization of receptor-tyrosine kinases, especially ErbB4 [55]. Those studies showed that the intracellular domain of ErbB4 is not only sorted to lysosomes and recycled to the cell membrane, it is also detected in nucleus, cytoplasm and mitochondria.

Our co-immunoprecipitation studies identified specific protein–protein interactions between ErbB4 and PSEN-1 and between ErbB4 and YAP in E17 type II cells. PSEN-1 and YAP antibodies each precipitated the full-length ErbB4 and the 4ICD. PSEN-1 associated with the full-length ErbB4 and its 80 kDa fragment, suggesting that γ-secretase alters the membrane associated 4ICD into a soluble form. It is unclear whether full-length ErbB4 or only the 4ICD moves into the cell as part of the NRG-induced signaling process, since we found that YAP was also associated with both ErbB4 species. However, PSEN-1 and YAP were not simultaneously associated with ErbB4, suggesting a sequence of processing events. As expected, NRG stimulation caused enhanced association of PSEN-1 with ErbB4 and of YAP with the 4ICD fragment and also increased phosphorylation of these proteins, supporting once more the model of the interrelationship between NRG stimulation and ErbB4 processing in the developing type II cell. Nuclear fractionation studies gave us additional insight into the fate of 4ICD and YAP. We found enhanced nuclear localization of both proteins early after NRG stimulation, which then returned to the baseline state, consistent with NRG-induced YAP shuttling of 4ICD into the nucleus.

We tested the role of γ-secretase processing of ErbB4 in the maturation of the surfactant system in fetal mouse type II cells using primary fetal type II cells isolated at E17 from HER4^{heart} mice rescued from embryonic lethality by expression of a human *ErbB4* cDNA under the control of the cardiac-specific α-MHC (myosin heavy chain) promoter [39]. We have previously described the lung phenotype of adult [11] and fetal [10] HER4^{heart} mice. Lack of ErbB4 in HER4^{heart} fetal lung cells has been previously confirmed by us [10], as has documentation of expressed wild-type human ErbB4 transfected into HER4^{heart} fetal type II cells (Zscheppang et al., submitted). Transfection of ErbB4-naive type II cells from HER4^{heart} (−/−) E17 animals with a mutant ErbB4 lacking the γ-secretase binding site allowed us to study the regulatory role of γ-secretase cleavage in ErbB4 signaling in type II cell surfactant protein expression. When compared to cells transfected with wild-type ErbB4, the increase of mRNA expression for *Sftpa*, *Sftpb*, and *Sftpd* was prevented by lack of the γ-secretase

cleavage site in ErbB4, indicating the critical need for γ-secretase cleavage of ErbB4 in the developing type II cells.

It is unclear why *Sftpa* actually decreased in cells transfected with the ErbB4 mutant compared to untransfected cells. We previously reported dynamic developmental changes between d17 and d18 in *Sftpa* mRNA expression in HER4^{heart} (−/−) mutant lungs [10]. Together, these findings suggest complex regulation of *Sftpa* expression in late fetal development. ErbB4 exists in isoforms that can and cannot be cleaved at the membrane, and with or without the chaperone-binding sequence for transport of the 80 kDa fragment. These different isoforms can have strikingly different effects in cells [31,56]. Thus, activation of alternate signaling pathways by ErbB4 isoforms not cleaved by PSEN-1 may result in inhibition of *Sftpa* expression. The lack of change in *Sftpc* after ErbB4 rescue may also indicate that alternate mechanisms support the expression of *Sftpc*, a possibility also consistent with our previous studies of the development of surfactant protein mRNA production in fetal HER4^{heart} mouse lungs [10]. The role of ErbB4 processing by PSEN-1 in promoting type II cell development is currently being addressed in more extensive studies of type II cell surfactant metabolism using siRNA knockdown of PSEN-1 in vitro [57].

In conclusion, these studies indicate that ErbB4 signaling in fetal lung type II cells utilizes the pathway of the PSEN-1-dependent γ-secretase proteolysis, followed by trafficking with YAP to the nucleus. γ-Secretase cleavage and nuclear transport are crucial for fetal lung type II cell surfactant protein mRNA production. Our results emphasize the importance of PSEN-1 and YAP for ErbB4 signaling in development and may provide significant clues for how to target ErbB4 biology in developing translational applications.

Supplementary materials related to this article can be found online at doi:10.1016/j.bbamcr.2010.12.017.

Acknowledgments

We thank Lucia Pham and Dagmar Stelte for their invaluable assistance. This work was supported by NIH HL037930, NIH HL085648, the Gerber Foundation, the Peabody Foundation, Susan B. Saltonstall Fund, Tufts Medical Center Research Fund, and Deutsche Forschungsgesellschaft DFG 378/3-2.

References

[1] M.E. Avery, J. Mead, Surface properties in relation to atelectasis and hyaline membrane disease, AMA J. Dis. Child. 97 (1959) 517–523.
[2] A.H. Jobe, M. Ikegami, Surfactant metabolism, Clin. Perinatol. 20 (1993) 683–696.
[3] C.E. Dammann, H.C. Nielsen, K.L. Carraway III, Role of neuregulin1b in the developing lung, Am. J. Resp. Crit. Care Med. 167 (2003) 1711–1716.
[4] K. Zscheppang, W. Liu, M.V. Volpe, H.C. Nielsen, C.E.L. Dammann, ErbB4 regulates fetal surfactant phospholipid synthesis in primary fetal rat type II cells, Am. J. Physiol. Lung Cell. Mol. Physiol. 293 (2007) 429–435.
[5] W. Liu, K. Zscheppang, S. Murray, H.C. Nielsen, C.E.L. Dammann, The ErbB4 receptor in fetal rat lung fibroblasts and type II cells, Biochim. Biophys. Acta 1772 (2007) 737–747.
[6] M. Gassmann, F. Casagranda, D. Orioll, H. Simon, C. Lai, R. Klein, G. Lemke, Aberrant neural and cardiac development in mice lacking the ErbB4 neuregulin receptor, Nature 378 (1995) 390–394.
[7] K.-F. Lee, H. Simon, H. Chen, B. Bates, M.-C. Hung, C. Hauser, Requirement for neuregulin receptor erbB2 in neural and cardiac development, Nature 378 (1995) 394–398.
[8] D. Meyer, C. Birchmeier, Multiple essential functions of neuregulin in development, Nature 378 (1995) 386–390.
[9] D. Riethmacher, E. Sonnenberg-Riethmacher, V. Brinkmann, T. Yamaai, G.R. Lewin, C. Birchmeier, Severe neuropathies in mice with targeted mutations in the ErbB3 receptor, Nature 389 (1997) 725–730.
[10] W. Liu, E. Purevdorj, K. Zscheppang, D. von Mayersbach, J. Behrens, M.-J. Brinkhaus, H.C. Nielsen, A. Schmiedl, C.E.L. Dammann, ErbB4 regulates the timely progression of late fetal lung development, Biochim. Biophys. Acta 1803 (2010) 832–839.
[11] E. Purevdorj, K. Zscheppang, H.G. Hoymann, A. Braun, D. von Mayersbach, M.-J. Brinkhaus, A. Schmiedl, C.E.L. Dammann, ErbB4 deletion leads to changes in lung function and structure similar to bronchopulmonary dysplasia, Am. J. Physiol. Lung Cell. Mol. Physiol. 294 (2008) L516–L522.
[12] K. Zscheppang, E. Korenbaum, W. Bueter, S. Ramadurai, H.C. Nielsen, C.E.L. Dammann, ErbB4 receptor dimerization, localization and co-localization in mouse lung type II epithelial cells, Pediatr. Pulmonol. 41 (2006) 1205–1212.
[13] C.-Y. Ni, M.P. Murphy, T.E. Golde, G. Carpenter, g-Secretase cleavage and nuclear localization of ErbB-4 receptor tyrosine kinase, Science 294 (2001) 2179–2181.
[14] M. Vecchi, J. Baulida, G. Carpenter, Selective cleavage of the heregulin receptor ErbB-4 by protein kinase C activation, J. Biol. Chem. 271 (1996) 18989–18995.
[15] W. Zhou, G. Carpenter, Heregulin-dependent trafficking and cleavage of ErbB-4, J. Biol. Chem. 275 (2000) 34737–34743.
[16] C. Rio, J.D. Buxbaum, J.J. Peschon, G. Corfas, Tumor necrosis factor-alpha-converting enzyme is required for cleavage of erbB4/HER4, J. Biol. Chem. 275 (2000) 10379–10387.
[17] Q.C. Cheng, O. Tikhomirov, W. Zhou, G. Carpenter, Ectodomain cleavage of ErbB-4: characterization of the cleavage site and m80 fragment, J. Biol. Chem. 278 (2003) 38421–38427.
[18] H.J. Lee, K.M. Jung, Y.Z. Huang, L.B. Bennett, J.S. Lee, L. Mei, T.W. Kim, Presenilin-dependent gamma-secretase-like intramembrane cleavage of ErbB4, J. Biol. Chem. 277 (2002) 6318–6323.
[19] A. Capell, J. Grunberg, B. Pesold, A. Diehlmann, M. Citron, R. Nixon, K. Beyreuther, D.J. Selkoe, C. Haass, The proteolytic fragments of the Alzheimer's disease-associated presenilin-1 form heterodimers and occur as a 100–150-kDa molecular mass complex, J. Biol. Chem. 273 (1998) 3205–3211.
[20] F. Chen, G. Yu, S. Arawaka, M. Nishimura, T. Kawarai, H. Yu, A. Tandon, A. Supala, Y.Q. Song, E. Rogaeva, P. Milman, C. Sato, C. Yu, C. Janus, J. Lee, L. Song, L. Zhang, P.E. Fraser, P.H. St George-Hyslop, Nicastrin binds to membrane-tethered Notch, Nat. Cell Biol. 3 (2001) 751–754.
[21] D. Edbauer, E. Winkler, J.T. Regula, B. Pesold, H. Steiner, C. Haass, Reconstitution of gamma-secretase activity, Nat. Cell Biol. 5 (2003) 486–488.
[22] W.P. Esler, W.T. Kimberly, B.L. Ostaszewski, T.S. Diehl, C.L. Moore, J.Y. Tsai, T. Rahmati, W. Xia, D.J. Selkoe, M.S. Wolfe, Transition-state analogue inhibitors of gamma-secretase bind directly to presenilin-1, Nat. Cell Biol. 2 (2000) 428–434.
[23] R. Francis, G. McGrath, J. Zhang, D.A. Ruddy, M. Sym, J. Apfeld, M. Nicoll, M. Maxwell, B. Hai, M.C. Ellis, A.L. Parks, W. Xu, J. Li, M. Gurney, R.L. Myers, C.S. Himes, R. Hiebsch, C. Ruble, J.S. Nye, D. Curtis, aph-1 and pen-2 are required for Notch pathway signaling, gamma-secretase cleavage of betaAPP, and presenilin protein accumulation, Dev. Cell 3 (2002) 85–97.
[24] Y.M. Li, M.T. Lai, M. Xu, Q. Huang, J. DiMuzio-Mower, M.K. Sardana, X.P. Shi, K.C. Yin, J.A. Shafer, S.J. Gardell, Presenilin 1 is linked with gamma-secretase activity in the detergent solubilized state, Proc. Natl. Acad. Sci. U. S. A 97 (2000) 6138–6143.
[25] G. Yu, M. Nishimura, S. Arawaka, D. Levitan, L. Zhang, A. Tandon, Y.Q. Song, E. Rogaeva, F. Chen, T. Kawarai, A. Supala, L. Levesque, H. Yu, D.S. Yang, E. Holmes, P. Milman, Y. Liang, D.M. Zhang, D.H. Xu, C. Sato, E. Rogaev, M. Smith, C. Janus, Y. Zhang, R. Aebersold, L.S. Farrer, S. Sorbi, A. Bruni, P. Fraser, P. St George-Hyslop, Nicastrin modulates presenilin-mediated notch/glp-1 signal transduction and betaAPP processing, Nature 407 (2000) 48–54.
[26] C. Goutte, M. Tsunozaki, V.A. Hale, J.R. Priess, APH-1 is a multipass membrane protein essential for the Notch signaling pathway in *Caenorhabditis elegans* embryos, Proc. Natl. Acad. Sci. U. S. A 99 (2002) 775–779.
[27] J. Omerovic, E.M. Puggioni, S. Napoletano, V. Visco, R. Fraioli, L. Frati, A. Gulino, M. Alimandi, Ligand-regulated association of ErbB-4 to the transcriptional co-activator YAP65 controls transcription at the nuclear level, Exp. Cell Res. 294 (2004) 469–479.
[28] S. Basu, N.F. Totty, M.S. Irwin, M. Sudol, J. Downward, Akt phosphorylates the Yes-associated protein, YAP, to induce interaction with 14-3-3 and attenuation of p73-mediated apoptosis, Mol. Cell 11 (2003) 11–23.
[29] F. Kanai, P.A. Marignani, D. Sarbassova, R. Yagi, R.A. Hall, M. Donowitz, A. Hisaminato, T. Fujiwara, Y. Ito, L.C. Cantley, M.B. Yaffe, TAZ: a novel transcriptional co-activator regulated by interactions with 14-3-3 and PDZ domain proteins, EMBO J. 19 (2000) 6778–6791.
[30] A. Komuro, M. Nagai, N.E. Navin, M. Sudol, WW domain-containing protein YAP associates with ErbB-4 and Acts as a co-transcriptional activator for the carboxyl-terminal fragment of ErbB-4 that translocates to the nucleus, J. Biol. Chem. 278 (2003) 33334–33341.
[31] S.P. Sardi, J. Murtie, S. Koirala, B.A. Patten, G. Corfas, Presenilin-dependent ErbB4 nuclear signaling regulates the timing of astrogenesis in the developing brain, Cell 127 (2006) 185–197.
[32] M. Volpe, K.T.W. Wang, H.C. Nielsen, M.R. Chinoy, Unique spatial and temporal expression patterns of Hoxa5, Hoxb4 and Hoxb6 in normal developing murine lung are modified in pulmonary hypoplasia, Birth Defects Res. A 82 (2008) 571–584.
[33] D. Villanueva, K. Wang, H.C. Nielsen, S.M. Ramadurai, Expression of specific protein kinase C isoforms and ligand-specific activation of PKCa in late gestation fetal lung, Exp. Lung Res. 33 (2007) 185–196.
[34] W. Bueter, O. Dammann, K. Zscheppang, E. Korenbaum, C.E. Dammann, ErbB receptors in fetal endothelium—a potential linkage point for inflammation-associated neonatal disorders, Cytokine 36 (2006) 267–275.
[35] P. Chomczynski, N. Sacchi, Single-step method of RNA isolation by acid guanidium thiocyanate–phenol–chloroform extraction, Anal. Biochem. 162 (1987) 156–159.
[36] A.N. Garratt, O. Voiculescu, P. Topilko, P. Charnay, C. Birchmeier, A dual role of erbB2 in myelination and in expansion of the schwann cell precursor pool, J. Cell Biol. 148 (2000) 1035–1046.
[37] D. Seiffert, J.D. Bradley, C.M. Rominger, D.H. Rominger, F. Yang, J.E. Meredith Jr., Q. Wang, A.H. Roach, L.A. Thompson, S.M. Spitz, J.N. Higaki, S.R. Prakash, A.P. Combs, R.A. Copeland, S.P. Arneric, P.R. Hartig, D.W. Robertson, B. Cordell, A.M. Stern, R.E. Olson, R. Zaczek, Presenilin-1 and -2 are molecular targets for gamma-secretase inhibitors, J. Biol. Chem. 275 (2000) 34086–34091.
[38] K. Furukawa, N. Pante, U. Aebi, L. Gerace, Cloning of a cDNA for lamina-associated polypeptide 2 (LAP2) and identification of regions that specify targeting to the nuclear envelope, EMBO J. 14 (1995) 1626–1636.

[39] H. Tidcombe, A. Jackson-Fisher, K. Mathers, D.F. Stern, M. Gassmann, J.P. Golding, Neural and mammary gland defects in ErbB4 knockout mice genetically rescued from embryonic lethality, Proc. Natl Acad. Sci. USA 100 (2003) 8281–8286.
[40] J. Shen, R.T. Bronson, D.F. Chen, W. Xia, D.J. Selkoe, S. Tonegawa, Skeletal and CNS defects in presenilin-1-deficient mice, Cell 89 (1997) 629–639.
[41] A. Herreman, D. Hartmann, W. Annaert, P. Saftig, K. Craessaerts, L. Serneels, L. Umans, V. Schrijvers, F. Checler, H. Vanderstichele, V. Baekelandt, R. Dressel, P. Cupers, D. Huylebroeck, A. Zwijsen, L.F. Van, S.B. De, Presenilin 2 deficiency causes a mild pulmonary phenotype and no changes in amyloid precursor protein processing but enhances the embryonic lethal phenotype of presenilin 1 deficiency, Proc. Natl. Acad. Sci. U. S. A 96 (1999) 11872–11877.
[42] P. Mastrangelo, P.M. Mathews, M.A. Chishti, S.D. Schmidt, Y. Gu, J. Yang, M.J. Mazzella, J. Coomaraswamy, P. Horne, B. Strome, H. Pelly, G. Levesque, C. Ebeling, Y. Jiang, R.A. Nixon, R. Rozmahel, P.E. Fraser, P. St George-Hyslop, G.A. Carlson, D. Westaway, Dissociated phenotypes in presenilin transgenic mice define functionally distinct gamma-secretases, Proc. Natl. Acad. Sci. U. S. A 102 (2005) 8972–8977.
[43] M.T. Lai, E. Chen, M.C. Crouthamel, J. DiMuzio-Mower, M. Xu, Q. Huang, E. Price, R.B. Register, X.P. Shi, D.B. Donoviel, A. Bernstein, D. Hazuda, S.J. Gardell, Y.M. Li, Presenilin-1 and presenilin-2 exhibit distinct yet overlapping gamma-secretase activities, J. Biol. Chem. 278 (2003) 22475–22481.
[44] E.M. Morin-Kensicki, B.N. Boone, M. Howell, J.R. Stonebraker, J. Teed, J.G. Alb, T.R. Magnuson, W. O'Neal, S.L. Milgram, Defects in yolk sac vasculogenesis, chorioallantoic fusion, and embryonic axis elongation in mice with targeted disruption of Yap65, Mol. Cell. Biol. 26 (2006) 77–87.
[45] P.H. Burri, Fetal and postnatal development of the lung, Annu. Rev. Physiol. 46 (1984) 617–628.
[46] P.H. Wen, V.L. Friedrich Jr., J. Shioi, N.K. Robakis, G.A. Elder, Presenilin-1 is expressed in neural progenitor cells in the hippocampus of adult mice, Neurosci. Lett. 318 (2002) 53–56.
[47] K. Uemura, A. Kuzuya, Y. Shimozono, N. Aoyagi, K. Ando, S. Shimohama, A. Kinoshita, GSK3beta activity modifies the localization and function of presenilin 1, J. Biol. Chem. 282 (2007) 15823–15832.
[48] J. Li, M. Xu, H. Zhou, J. Ma, H. Potter, Alzheimer presenilins in the nuclear membrane, interphase kinetochores, and centrosomes suggest a role in chromosome segregation, Cell 90 (1997) 917–927.
[49] S.J. Jeong, H.S. Kim, K.A. Chang, D.H. Geum, C.H. Park, J.H. Seo, J.C. Rah, J.H. Lee, S.H. Choi, S.G. Lee, K. Kim, Y.H. Suh, Subcellular localization of presenilins during mouse preimplantation development, FASEB J. 14 (2000) 2171–2176.
[50] G.G. Van, W. Annaert, B.C. Van, Binding partners of Alzheimer's disease proteins: are they physiologically relevant? Neurobiol. Dis. 7 (2000) 135–151.
[51] A.L. Parks, D. Curtis, Presenilin diversifies its portfolio, Trends Genet. 23 (2007) 140–150.
[52] K. Dillen, W. Annaert, A two decade contribution of molecular cell biology to the centennial of Alzheimer's disease: are we progressing toward therapy? Int. Rev. Cytol. 254 (2006) 215–300.
[53] J. Kim, S. Hamamoto, M. Ravazzola, L. Orci, R. Schekman, Uncoupled packaging of amyloid precursor protein and presenilin 1 into coat protein complex II vesicles, J. Biol. Chem. 280 (2005) 7758–7768.
[54] D. Selkoe, R. Kopan, Notch and presenilin: regulated intramembrane proteolysis links development and degeneration, Annu. Rev. Neurosci. 26 (2003) 565–597.
[55] G. Carpenter, H.J. Liao, Trafficking of receptor tyrosine kinases to the nucleus, Exp. Cell Res. 315 (2009) 1556–1566.
[56] R.S. Muraoka-Cook, M.A. Sandahl, K.E. Strunk, L.C. Miraglia, C. Husted, D.M. Hunter, K. Elenius, L.A. Chodosh, H.S. Earp III, ErbB4 splice variants Cyt1 and Cyt2 differ by 16 amino acids and exert opposing effects on the mammary epithelium in vivo, Mol. Cell. Biol. 29 (2009) 4935–4948.
[57] A. Ritzkat, E. Pringa, C. Scapin, O. Guengoeze, M. Dere, M.V. Volpe, C.E.L. Dammann, H.C. Nielsen, Knock-down of presenilin-1 blocks ErbB4-regulated surfactant synthesis in MLE-12 cells, E-PAS (2010) 3701.21.